

THE EFFECTS OF FIBER CONCENTRATION AND FIBER DIMENSIONS ON THE
SEDIMENTATION OF A SPHERE IN FIBER-FILLED HYDRAULIC FRACTURING
FLUIDS

Undergraduate Research Thesis

Presented in partial Fulfillment of the Requirements for Graduation with Research Distinction in
the College of Engineering of The Ohio State University

By

Tiara Ann Maula

William G. Lowry Department of Chemical and Biomolecular Engineering

2016

Thesis Committee:

Dr. Kurt W. Koelling, Advisor

Dr. Jacques Zakin

Copyright by

Tiara Ann Maula

2016

Abstract

Industrialization has created a tremendous energy demand. Coupled with instability in the Middle East, the depletion of conventional oil reserves, and the development of horizontal drilling, the renewed need for hydrocarbons has led to the widespread adoption of hydraulic fracturing (“fracking”). Fracking uses high pressure fluid to fracture shale deep under the ground. To increase the permeability of shale, sand-like proppant particles are added to the fluid, necessitating the use of viscosifying agents and other chemical additives to retard proppant sedimentation. Since certain additives used in fracking fluids are hazardous, specifically the crosslinker sodium tetraborate, concerns over the environmental sustainability of fracking proliferate. Among them is fracking's potential for contaminating groundwater reserves. Previous research has found that adding a small concentration of fibers into fracking fluids allows for a reduction in crosslinker loading while achieving similar proppant retardation effects. In this research, experiments were conducted to study the effect of fiber dimensions and concentration on the sedimentation velocity of proppant particles in fiber-filled fracking fluids. Furthermore, this research has resulted in a computational model for predicting the settling velocity of a sphere which accounts for the presence and dimension of fibers. And while most proppants are aspherical, knowing the settling behavior of spherical particles are still instructive. In the flow regime experimentally observed in this research, sphere sedimentation models developed for power-law fluids are applicable for similar circumstances in fracking fluids, and the presence of fibers can be accounted for by performing a momentum and energy balance on sphere-fiber interactions. The purpose of this research is to determine the optimal fiber properties for fracking applications and streamline the process of searching for the appropriate fiber given certain rheological properties of a fluid. This research is not only relevant to making fracking more

efficient and environmentally safer, this research is also relevant to the paper manufacturing and concrete reinforcement industries.

Acknowledgements

I would like to thank Dr. Kurt Koelling for his guidance, patience, and encouragement throughout this project. I also would like to thank Ziwei Wang, Xutao Shi, and Joseph Gauthier for their support.

Vita

2016.....B.S. Chemical and Biomolecular Engineering, The Ohio State University

Field of Study

Major Field: Chemical Engineering

Table of Contents

Abstract.....	i
Acknowledgements.....	iii
Vita.....	iv
Field of Study.....	iv
List of Figures.....	vii
List of Tables.....	viii
Chapter 1: Introduction.....	1
1.1 Motivation.....	1
1.2 Background.....	2
1.1 Preliminary Findings.....	5
Chapter 2: Experimental Methods.....	10
Chapter 3: Results and Discussion.....	13
3.1 Settling velocity experiments.....	13
3.2 Rheology of hydraulic fracturing fluids.....	18
3.2 Modeling settling velocity in fiberless fluid.....	20
3.3 Modeling the effect of fibers.....	24
Chapter 4: Conclusions and Future Work.....	29
4.1 Conclusions.....	29
4.2 Future work.....	30

References..... 31

List of Figures

Figure 1	2
Figure 2	3
Figure 3	4
Figure 4	5
Figure 5	6
Figure 6	7
Figure 7	8
Figure 8	8
Figure 9	11
Figure 10	14
Figure 11	15
Figure 12	17
Figure 13	17
Figure 14	18
Figure 15	20
Figure 16	24
Figure 17	25
Figure 18	27
Figure 19	27

List of Tables

Table 1	12
Table 2a.....	12
Table 2b	12
Table 3	23

List of Symbols

d	Fiber diameter
L	Fiber length
E	Modulus of elasticity of the fiber
W	Net weight of the sphere
η	Fluid viscosity
η_0	Zero-shear viscosity
η_∞	Viscosity at very high shear
n	Flow index
k	Consistency index
$\dot{\gamma}_{max}$	Maximum shear rate around the sphere
v	Velocity of the sphere
ρ_s	Density of the sphere
ρ_f	Density of the fluid
μ_f	Fluid viscosity
g	Acceleration due to gravity
R	Radius of the sphere
C_D	Drag coefficient of the sphere
Re	Reynolds number
$\dot{\gamma}_{avg}$	Average shear rate
m	Mass of the sphere
v_i	Initial velocity of the sphere

v_f	Final velocity of the sphere
m_c	Mass of the fiber
v_c	Translational velocity of the fiber
I_c	Moment of inertia of the fiber
ω_c	Angular velocity of the fiber
N_{hit}	Number of fibers hit
$V_{travelled}$	Volume travelled by the sphere
N_{fibers}	Total number of fibers in the system
V_{total}	Total volume of the system
r_{sphere}	Radius of the sphere
$r_{graduated\ cylinder}$	Radius of the graduated cylinder

Chapter 1: Introduction

1.1 Motivation

Hydraulic fracturing (“fracking”) is an increasingly popular means of obtaining hydrocarbons, facilitated by the global trend towards industrialization and the instability of the major oil producing nations. The development of horizontal drilling has made hydraulic fracturing an economically feasible means of obtaining hydrocarbons. But despite its promise of energy independence—U.S. shale gas reserves hold the equivalent of roughly 102 billion barrels worth of crude oil—many object to the practice of fracking, citing doubts about its environmental sustainability and its hazards to groundwater reservoirs [1][2].

However, shale gas is a great energy resource that will not remain unused so efforts should be made to make hydraulic fracturing more efficient and more environmentally sustainable. It has been found that adding fibers to hydraulic fracturing fluids allows for reduced loadings of certain chemical additives while maintaining the fluid’s rheological properties and transport capabilities [2][3][4].

One goal of this project to investigate how the physical properties of fibers affect sedimentation in hydraulic fracturing fluids. Another goal is to obtain a model relating the physical properties of the fiber and the fluid to the sedimentation velocity of an individual sphere. Ultimately, such a model could be used to predict the optimal fiber properties for enhancing a suspension of particles in any given fluid. Thus, this research is relevant to concrete reinforcement, composites manufacturing, and paper manufacturing in addition to hydraulic fracturing.

1.2 Background

Hydraulic fracturing is a hydrocarbon capturing technique. It extracts natural gas by drilling into organic rich shales thousands of feet beneath the ground and then pumping fluids to fracture the shale and release the gas. The fluids are then pumped back up the well in order to facilitate the transport of hydrocarbons. A schematic of the fracking process is show in Figure 1 below.

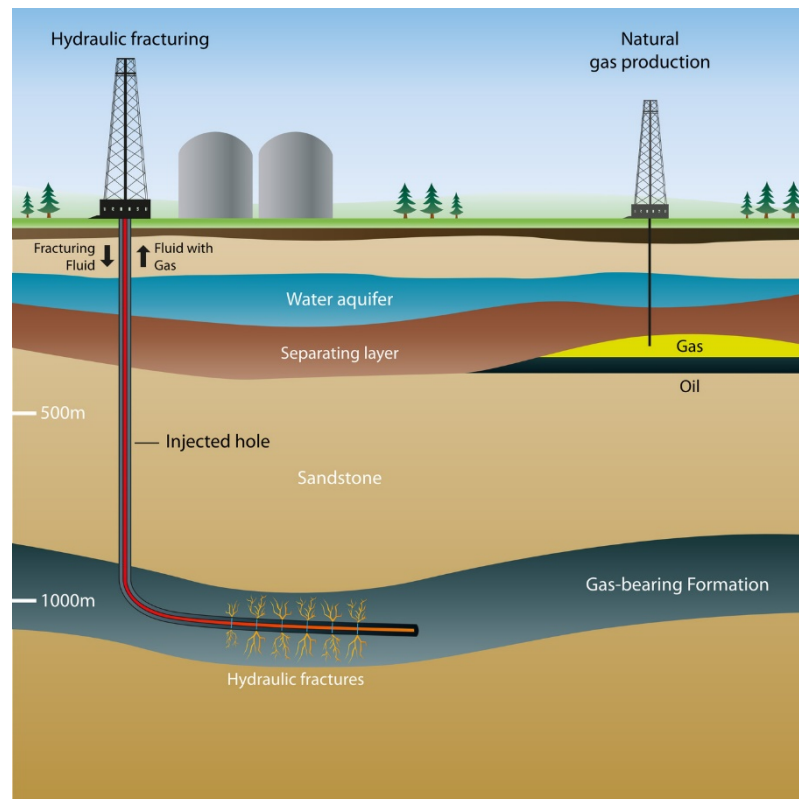


Figure 1. A schematic of hydraulic fracturing. [5]

In order for hydraulic fracturing to extract a sufficient amount of natural gas, small particles called proppants are added into the fracking fluid to keep the fractures open [2]. An illustration of this is shown in Figure 2. Figure 2a, shows how proppant settling affect the fracture height, and Figure 2b shows the effect of proppant distribution on the fracture faces. The majority of

proppants used in industry is 20/40 mesh sand. Gravitational forces cause the sedimentation of these proppants, resulting in an uneven distribution of proppants along the fractures and poor proppant transport in general, due to some proppants settling before reaching the full length of the fracture. Proppants are also necessary for extending the length of fractures in the shale, which is necessary because the tip of the fractures provide little to no hydrocarbon gain [2,6].

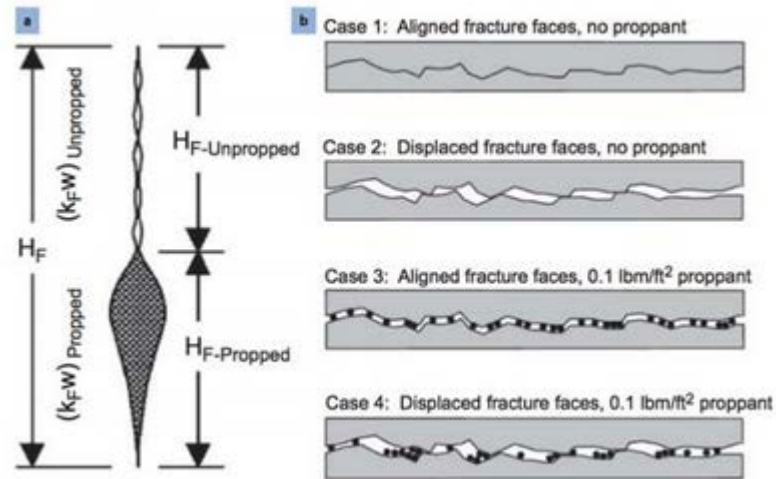


Figure 2. The effect of proppants on fracture geometry. [6]

To prevent proppant sedimentation, viscosifiers are added into the fracking fluid. The most commonly used viscosifier is high molecular weight hydroxypropyl guar (HPG), composed of long chains of mannose and galactose sugars [7]. Guar and its derivatives have a molecular weight of approximately 10^5 - 10^6 g/mol [7]. Crosslinkers are added to the fracking fluids to further increase its viscosity, and it has been found that a crosslinked guar solution prevents proppant sedimentation better than uncrosslinked guar solution [2]. Borate ions, although not the most effective crosslinker, are the most commonly used crosslinker for guar, and sodium

tetraborate is a typical source of borate ions [7]. The molecular structure of crosslinked guar is shown in Figure 3. Borate ions form complexes with the hydroxyl groups, linking guar molecules together.

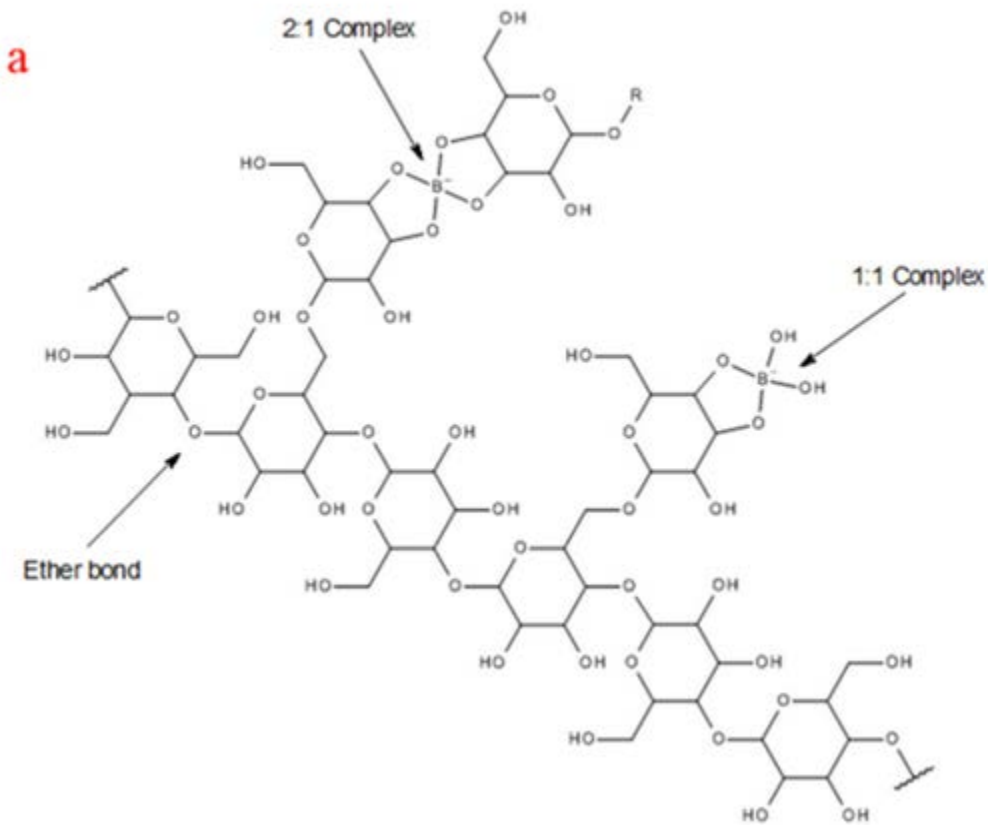


Figure 3. The molecular structure of crosslinked guar [6].

In addition to the crosslinker sodium tetraborate being an environmental and health hazard, the addition of viscosifiers into fracking fluids also pose the further disadvantage of decreasing the permeability of the fracture through the formation of a layer of filter cake and also of increasing the energy requirements to pump the fluids back up the well to capture the hydrocarbons [2].

Ideally therefore fracking fluids should have a low viscosity and yet be able to retard proppant sedimentation.

1.1 Preliminary Findings

It has been reported that the addition of a small amount of fibers improve proppant transport [7, 6 2]. These have been confirmed by experiments on the settling velocity of a PTFE particle in guar-borate solution (see Figure 4 below). A sphere was used instead of a sand particle to ensure that the irregular projection area of sand do not bias the results. These experiments show that small concentrations of chopped nylon fibers, on the order of 10^{-2} wt %, reduces the settling velocity of an individual sphere more effectively than a comparable amount of crosslinker (CL).

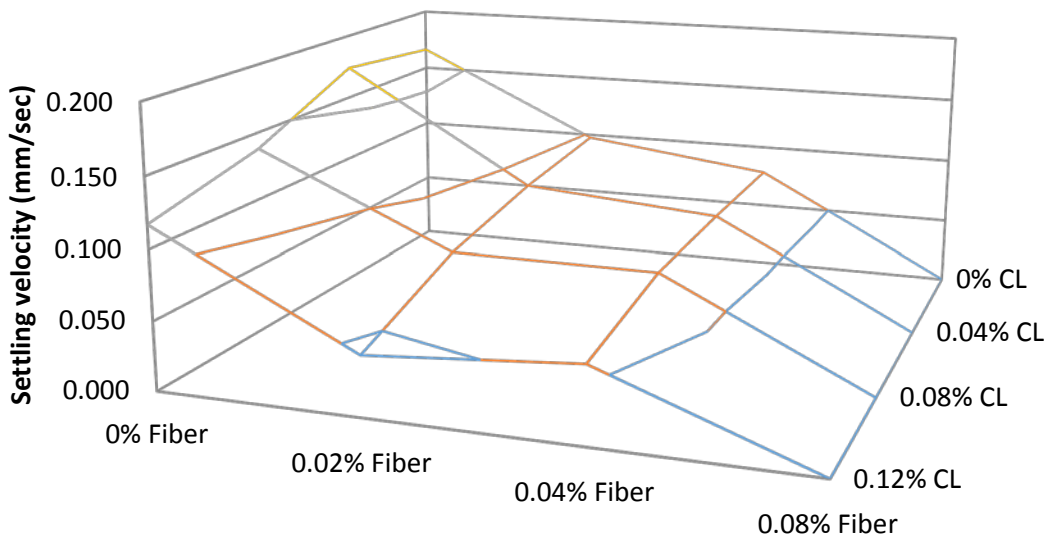


Figure 4. The effects of fiber concentration and crosslinker concentration on the settling velocity of a spherical PTFE particle. [8]

Experiments have also confirmed findings that low fiber concentrations have a negligible effect on the rheological properties of the fracking fluid. A graph of the viscosity vs shear rate of a guar-borate solution for three different fiber concentrations are show in Figure 5 on the next page. It can be seen that the shear viscosity behavior for 0.08 wt % fiber solution is identical to the shear viscosity behavior of 0.0 wt % fiber solution.

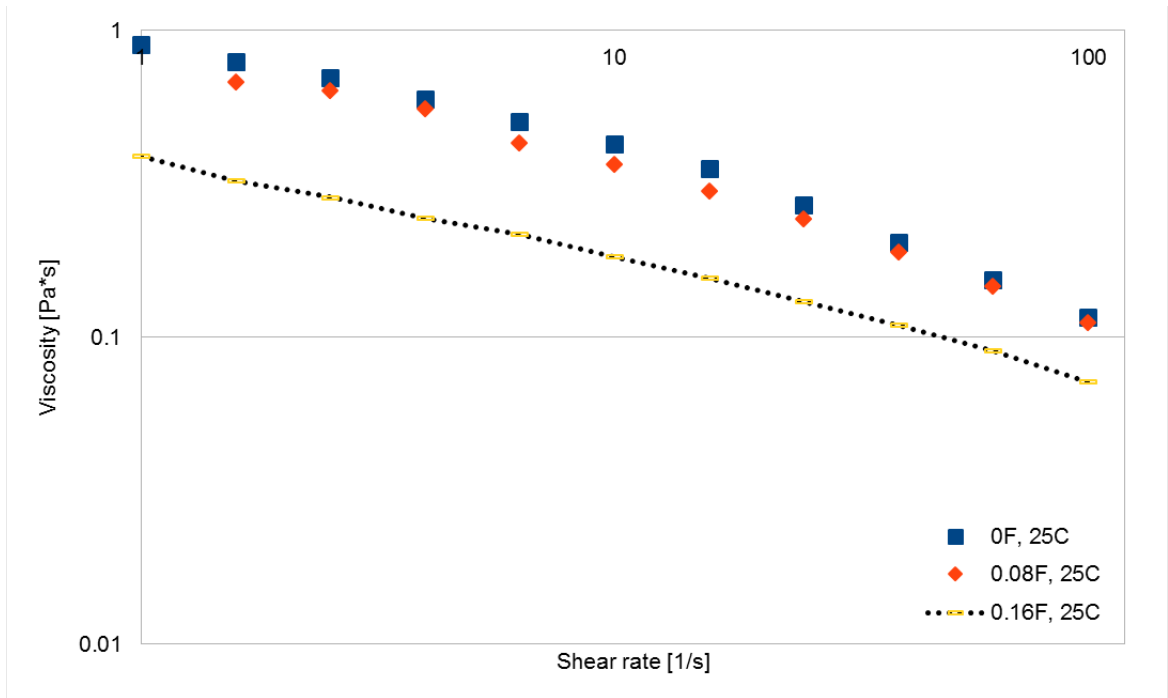


Figure 5. Small concentrations of carbon fiber ($d = 7 \pm 2 \mu\text{m}$, $L = 200\text{-}300 \mu\text{m}$) have a negligible effect on the viscosity of guar borate solution.

Furthermore, it has been found from experiments investigating the effect of fiber concentration on the settling velocity of a sphere that different fibers affect settling rate differently. For example Figure 4 shows that for 1 cm nylon multimesh fibers, the settling velocity of a 2.2 g/cc, 1.06 cm diameter sphere increases when the fiber concentration is increased from 0.02 to 0.04 wt %, and that the settling velocity is 0 mm/s for 0.08 wt % fiber. On the other hand, Figure 6 shows

that for very short, very thin pitch-based carbon fibers ($d = 7 \pm 2 \mu\text{m}$, $L = 200\text{-}300 \mu\text{m}$), there tends to be an optimal fiber concentration around for reducing settling velocity in guar-borate solution at 25°C , and that the settling velocity does not reach 0 mm/s even at $0.16 \text{ wt } \%$ fiber concentration. Settling velocity experiments were also conducted using these same type of carbon fibers and the same 1.06 g/cc sphere in $2 \text{ wt } \%$ polyethylene oxide (PEO) solution, and an optimal fiber concentration can still be observed. The results of this experiment is summarized in Figure 7. PEO is a simple polymer used as a model system in order to determine that the unexpected behavior found in Figure 6 is not due to crosslinking.

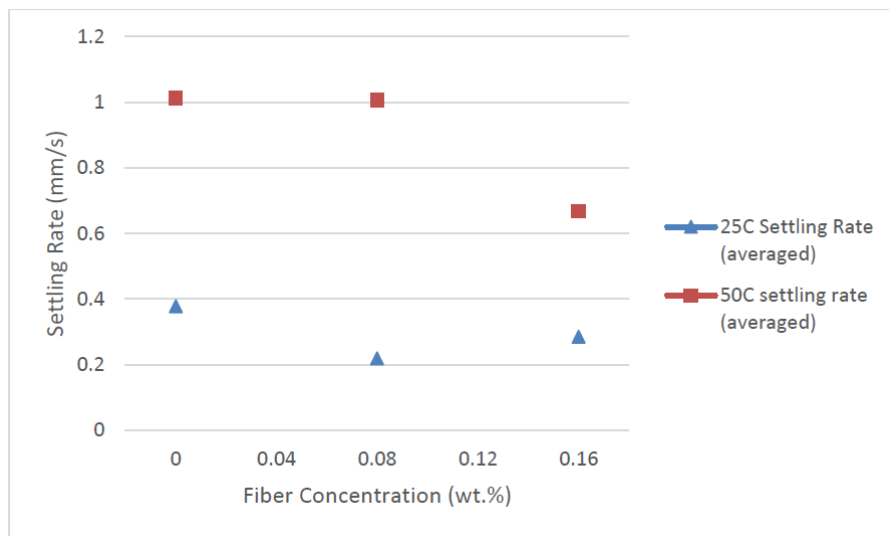


Figure 6. The effect of $0.2\text{-}0.3 \text{ mm}$ carbon fiber concentration on the settling velocity of a 1.06 g/cc , sphere in guar-borate solution. [9]

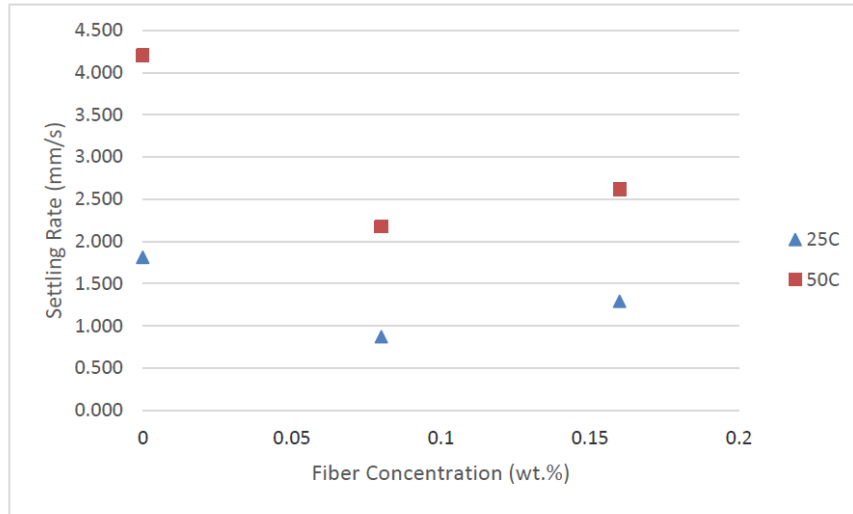


Figure 7. The effect of 0.2-0.3 mm carbon fiber concentration on the settling velocity of a 1.06 g/cc sphere in 2 wt % PEO solution. [9]

However, experiments conducted using 2 cm of nylon multimesh fibers and a 1.06 g/cc sphere have shown that settling rate always decreases as the fiber concentration is increased and that the settling velocity reaches 0 mm/s at 0.16 wt % fiber. This trend can be seen in Figure 8.

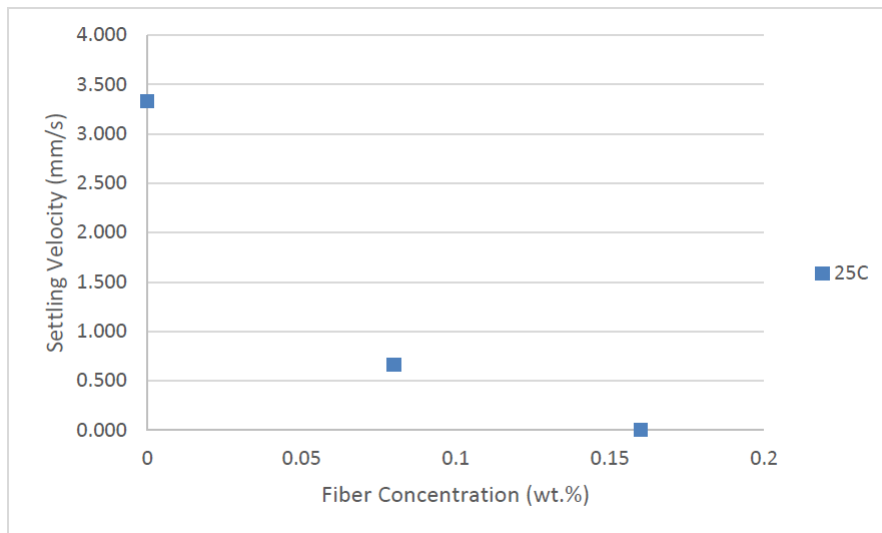


Figure 8. The effect of 2 cm nylon fiber concentration on the settling velocity of a 1.06 g/cc, 2 wt % PEO solution. [9]

These experiments show that the physical properties of the fiber, in addition to the concentration of fibers, affect settling velocity. By investigating more thoroughly how the physical properties of the fiber affect settling rate, hydraulic fracturing processes could be made more environmentally and economically efficient. Such information will aid in selecting fibers which require the least mass concentration because their effect on settling velocity is maximized. In this project the, effects of the physical properties of a fiber on the settling velocity of a single sphere settling in a fracking fluid was investigated, and a computational model has been developed in order to predict the settling velocity of a given sphere provided the rheological characteristics of the fluid and physical characteristics of the fiber.

Chapter 2: Experimental Methods

Measuring the settling rates of proppant aggregates in fiber-filled fracking proved to be a challenging task. Proppants would tend to get caught in the fibers and would drag the fibers down to the bottom with them. This made it difficult to get an accurate picture how fast proppants actually settle. In some regions, some proppants continued to be suspended in the fluid even while the majority have already settled. This is dependent upon the orientation and distribution of fibers, which cannot be controlled for. Simpler experiments have therefore been devised where instead of using a certain mass concentration of proppants, an individual particle was used. This particle was chosen to be a sphere to ensure consistent particle mass and projection area.

In order to begin these simpler experiments, batch fluids have to be prepared first. Water is added into a blender, and the required amount of hydroxypropyl guar (0.5 wt %, molecular weight unknown but estimated to be in the order of 10^6) was incrementally added into the water, blending the solution through the application of small pulses at each incremental addition until it has dissolved. Once all the guar was completely dissolved, this same process is repeated for the required amount of sodium tetraborate (0-0.12 wt %).

The batch of fluid was then left stirring on a magnetic stirrer overnight until all bubbles in the fluid were dissipated and also to ensure that the solution was homogeneous. The batch fluid was then divided into 100 mL samples in mason jars, and a smaller sample was saved for rheological testing.

A predetermined amount of fibers were gradually added into each sample as required. As the fibers were added, the sample was continually stirred using a magnetic stirrer to ensure a homogenous dispersion of fibers. Once a homogenous fiber distribution was obtained, each sample was transferred to its own 100 mL graduated cylinder.

The settling tests were conducted by dropping a bead as closely as possible to the center of the graduated cylinder and filming its progress using a video camera. The settling velocity was obtained by analyzing the videos and measuring the time it took for a sphere to traverse a 19 mm interval (the tick marks on the graduate cylinders). After each trial, the samples were stirred to ensure that the reorientation of fibers which occurred when the sphere flowed past them did not affect the ensuing settling velocity measurements. Figure 9 below shows the experimental set up.

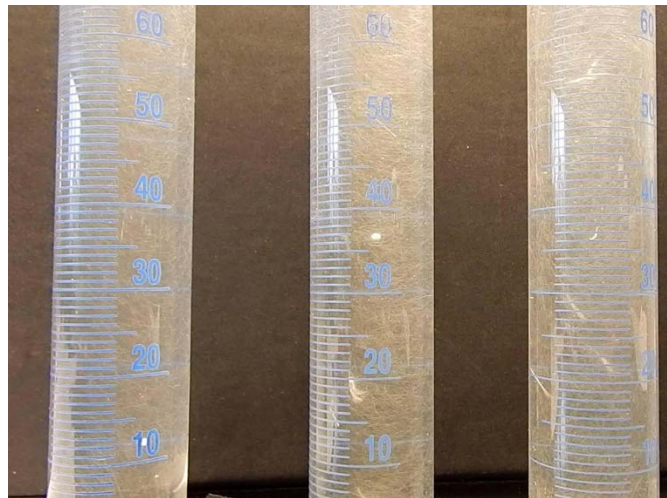


Figure 9. Experimental setup.

Experiments testing the effect of fiber dimensions were conducted using two different sphere particles and four different types of fiber. A table of the physical properties of the particles used

can be seen in Table 1 and a table of the physical properties of the different fibers used can be seen on Tables 2a and 2b.

Table 1. Spherical particles used in experiments.

Particle Type	Diameter [mm]	Density [g/cc]	Net Weight [N]
Aluminum (Al)	1	2.7	5.24E-05
Polytetrafluoroethylene (PTFE)	1.6	2.2	1.51E-04

Table 2a. Fibers used in the experiments.

Fiber	Material	Length [mm]	Diameter [um]
MM-6	Nylon	6	38
PP-6	Polypropylene	6	25
PP-4	Polypropylene	4	25
GL-6	Glass	6	13

Table 2b. Fibers used in the experiments.

Fiber	Material	Density [g/cc]	Elastic Modulus
MM-6	Nylon	1.13	3.00E+08
PP-6	Polypropylene	0.92	4.60E+09
PP-4	Polypropylene	0.92	4.60E+09
GL-6	Glass	2.6	6.50E+10

Rheological tests were also conducted for every base fluid created. These tests were conducted at room temperature. Steady-shear tests were conducted using a TA Instrument Ares LS-2 rotational rheometer with a parallel plate geometry (50 mm diameter, 0.5 mm gap) and shear rates ranging from 0.01 to 400 1/s. Small amplitude oscillatory shear tests were also conducted at the same geometry using angular frequencies in the range of 0.1 to 100 rad/s.

Chapter 3: Results and Discussion

3.1 Settling velocity experiments

Settling velocity experiments were conducted for the four different fiber types (see Tables 2a and 2b). In these experiments, fiber concentration was measured in the number of fibers, which was obtained from dividing the total volume of the fibers by the volume of an individual fiber. The total volume of fibers was obtained by dividing the total mass of the fibers by the density of the fiber.

The settling velocity results for the aluminum beads are found on Figure 13 below. The settling velocity results for the PTFE beads are found on Figure 13 on the next page. The physical properties of beads can be found in Table 1 on page 12.

In both cases, nylon fibers ($L = 6 \text{ mm}$, $d = 38 \text{ }\mu\text{m}$) were found to be the most effective for reducing settling rate, followed by glass ($L = 6 \text{ mm}$, $d = 13\mu\text{m}$). Polypropylene fibers of either length $L = 6 \text{ mm}$ or $L = 4 \text{ mm}$ and $d = 25 \text{ }\mu\text{m}$ are found not to reduce settling velocity. The 6 mm polypropylene fibers sometimes results in velocities faster than fracking fluids with zero fibers, and the 4 mm polypropylene fibers do not affect settling velocity.

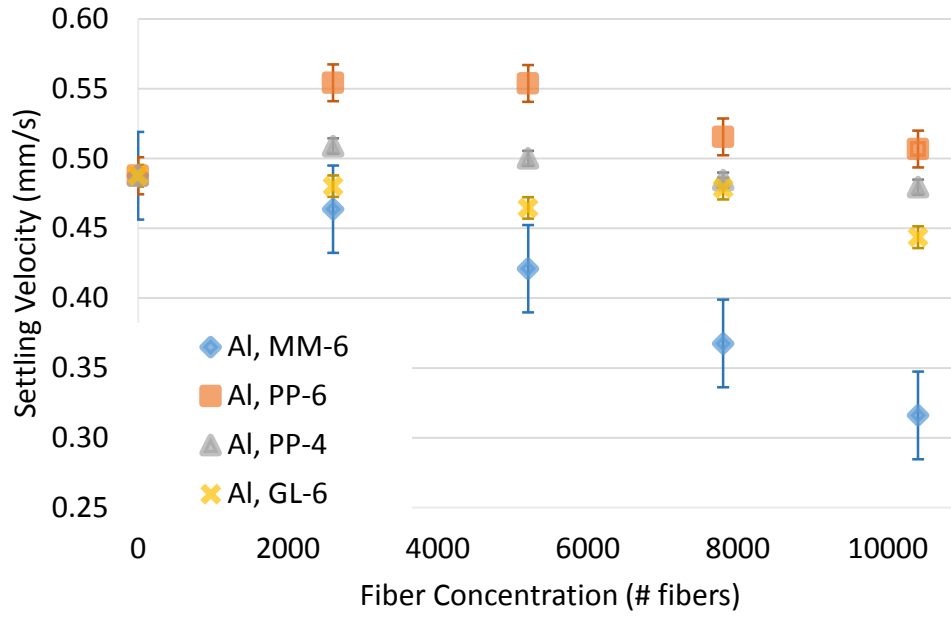


Figure 10. Settling velocities of aluminum particle.

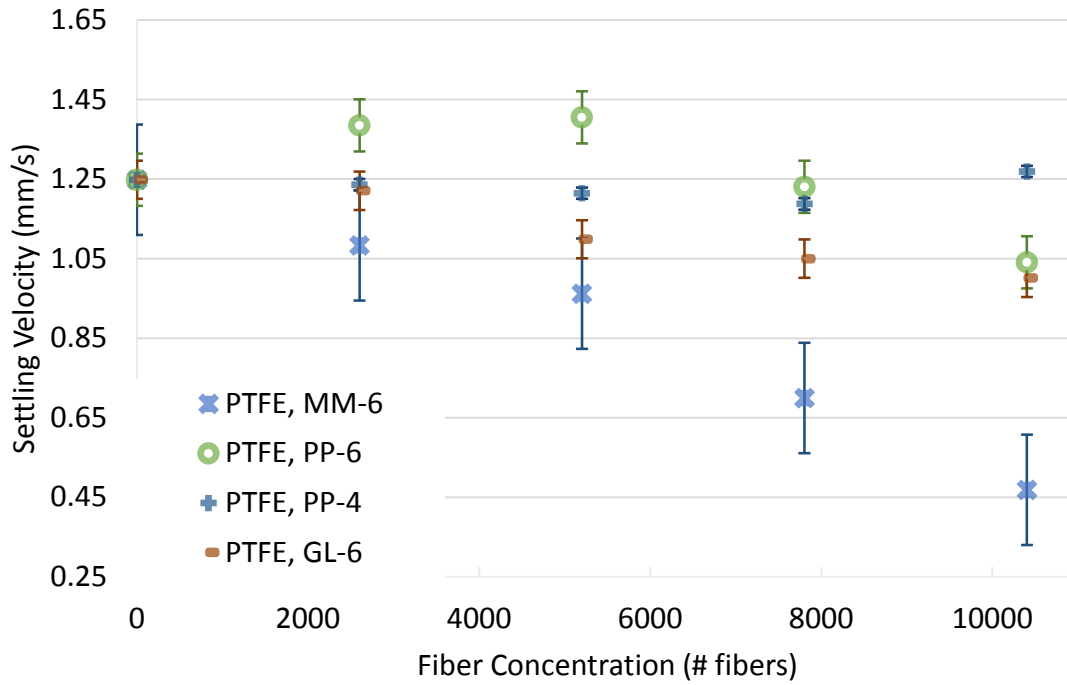


Figure 11. Settling velocities of PTFE particle.

In Figures 10 and 11, it is difficult to see the trends due to the physical properties of the fibers because of the variety of the fibers used. Thus the overall effect of the physical characteristics of the fiber were measured using the bending radius (R_{bend}), which is a function of fiber diameter, density, modulus of elasticity, and also of the net weight of the spherical particle it comes into contact with. It is an estimate of the bending undergone by a fiber in solutions where there is a high enough concentration of fibers. The expression for the bending radius is

$$R_{bend} = \frac{E\pi d^4}{64WL} \quad (1)$$

The assumption behind the bending radius is that it is valid only for small deformations and that one end of the fiber is stationary and the other end makes contact with the moving sphere [10].

The settling velocity vs the bending radius for the two different beads can be found on Figure 12 and Figure 13.

It can be seen from the two graphs that the settling velocity of the bead in fiber-filled fluid approaches the velocity in fiberless fluids at higher bending radii. When a fiber undergoes higher bending radii, it becomes less effective at blocking the path of the sphere. Also at high bending radii, fiber concentration begins to have little effect on settling velocity. Therefore, the optimal fiber type to be used for retarding particle sedimentation should have a low bending radius because it is where the effect of the fibers are most significant. It would be more efficient to use low concentrations of fiber with low bending radii, than high concentrations of fiber with high bending radii.

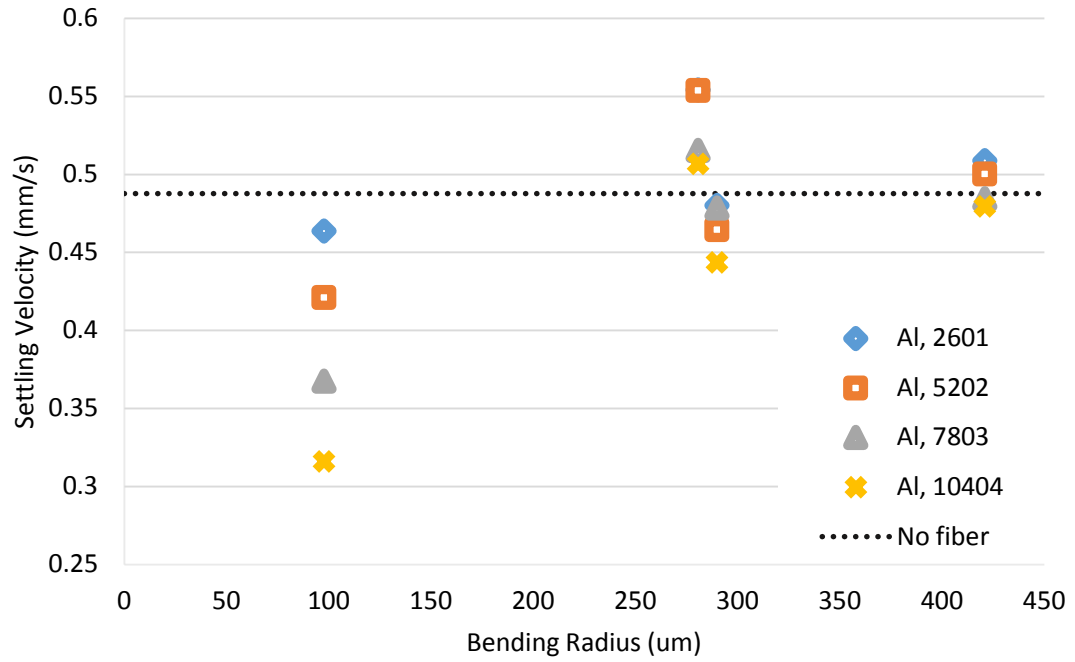


Figure 12. Settling velocities vs bending radius for aluminum particle.

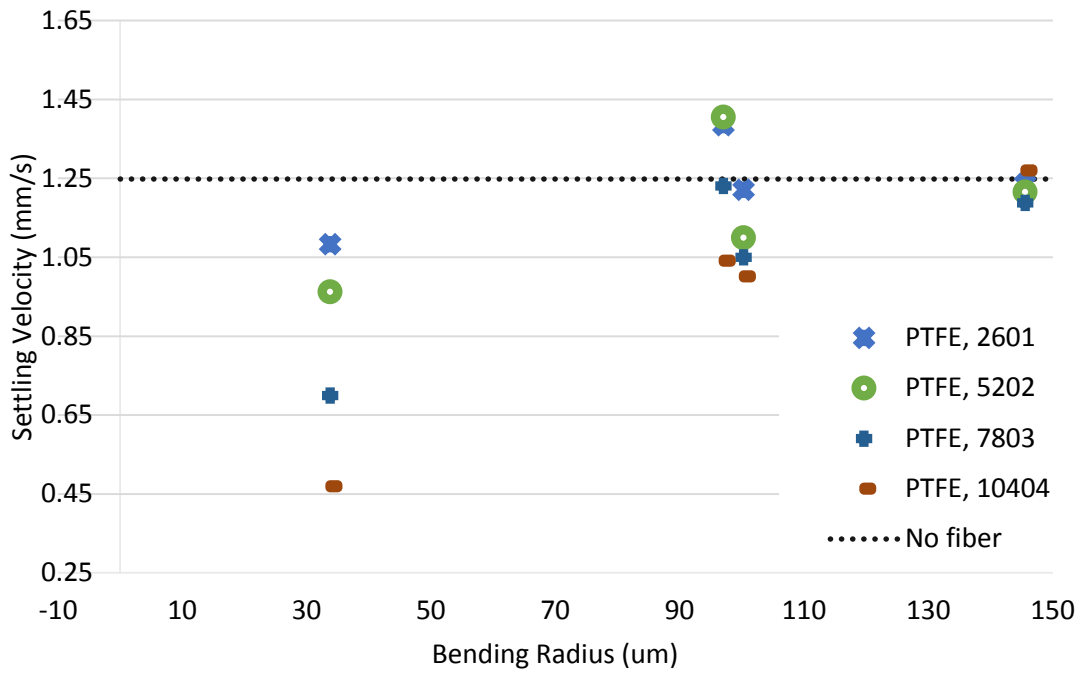


Figure 13. Settling velocities vs bending radius for PTFE particle.

The trends seen in Figures 10, 11, 12, and 13 could not be due entirely to the effect of fibers however. Polymers of high molecular weight degrade with shear, and the samples filled with fibers which are difficult to disperse were left in the stirrers longer, and the control sample and the sample used for rheological testing did not undergo the additional step of being stirred for the dispersion of fibers. However, polypropylene fibers were also the easiest to disperse and they had the least effect on the effective viscosity, so it is also possible that stirring the gels did not impart enough shear to cause degradation of the guar.

3.2 Rheology of hydraulic fracturing fluids

Hydraulic fracturing fluids are non-Newtonian, meaning their viscosity does not remain constant with respect to shear. Hydraulic fracturing fluids are in fact shear-thinning, and this behavior can be seen in Figures 14. The apparent viscosity of shear-thinning fluids decreases when subjected to an increase in shear. Shear-thinning behavior is common to many polymeric solutions.

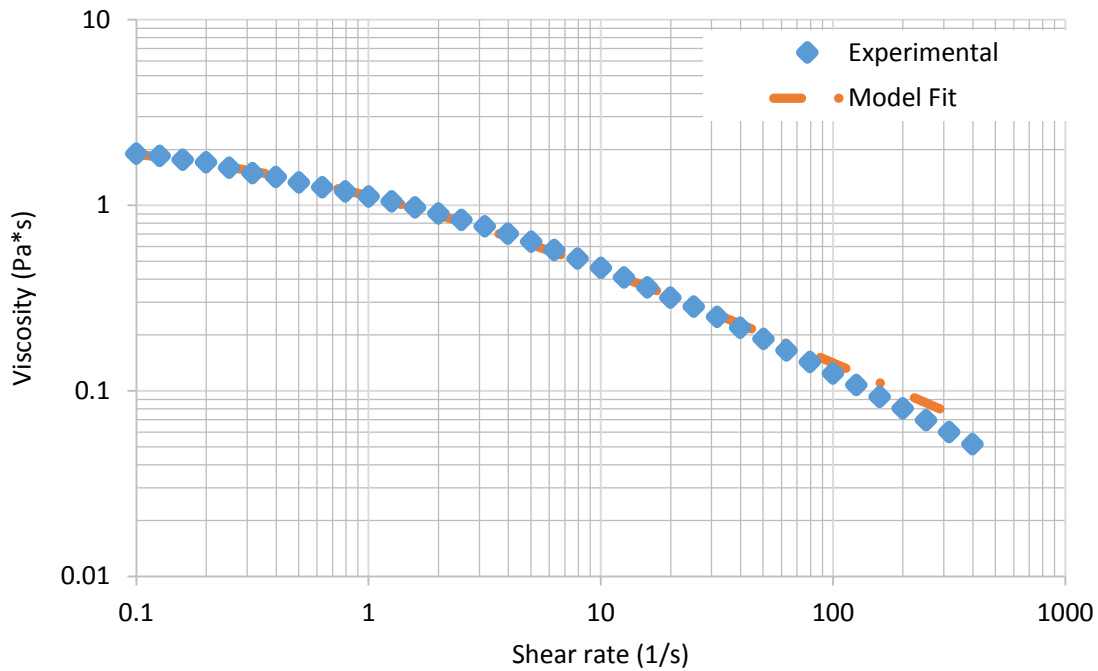


Figure 14. Hydraulic fracturing fluids are shear-thinning (0.5 % guar, 0.08 wt % sodium tetraborate solution).

Using least squares regression, a Cross model was fitted to the above data. The expression for the cross model is

$$\eta = \eta_{\infty} + \frac{\eta_0 - \eta_{\infty}}{1 + (k\dot{\gamma})^{1-n}} \quad (3)$$

Where η_0 is the zero-shear viscosity, η_∞ is the viscosity at very high shear. In the Cross model, the fluid is assumed to behave like a Newtonian fluid at very high and very low shear, and like a power-law fluid at intermediate shears; n and k are the fitting parameters for this power law region. In the base fluid used for these experiments, the Cross parameters were found to be $\eta_0 = 2.52 \text{ Pa}\cdot\text{s}$, $\eta_\infty = 0.001$, $n = 0.433$, $k = 1.47$, and the sum of all residuals was found to be 0.013. As can be seen in Figure 14, the Cross model provides a very good fit for the data up until shear rates of approximately 60 1/s. An estimate of the maximum shear rate, $\dot{\gamma}_{\max}$, around the aluminum and PTFE particles was made using Stoke's drag solution, show in Equation 4 below, where v is the sphere velocity and d is the sphere diameter [11].

$$\dot{\gamma}_{\max} = \frac{3v}{2d} \quad (3)$$

Using the experimental terminal velocities of the beads, it was found that the aluminum bead had a maximum shear rate of 1.5 1/s and the PTFE bead had 2.3 1/s. Both are an order of magnitude lower than the shear rate at which the Cross model begins to fail. So the Cross model provides an adequate description of the fluid at the shear rates which are experimentally encountered.

Another characteristic of hydraulic fracturing fluids are viscoelasticity, which means they recover from deformation. The viscoelasticity of the fluid can be measured by the storage (G') and loss (G'') moduli. The storage modulus is a measure of how much a material behaves like a Hookean solid, which recovers deformation perfectly; and the loss modulus is a measure of how much a material behaves like a Newtonian liquid, which does not store any energy from deformation [12]. The storage and loss moduli of a fluid could be obtained by performing small amplitude oscillatory shear tests using a rotational rheometer. In this test, a small amplitude

sinusoidal shear is applied to the fluid sample, and the stress is measured by the rheometer. The in-phase element of the stress is G' , and the out-of-phase element is G'' . An example of data collected from this test is shown in Figure 15. Figure 15 show that hydraulic fracturing fluids are viscoelastic, and that it has an elastic component (shown by G') and a viscous component (shown by G''). As the frequency is increased, the fluid becomes more elastic.

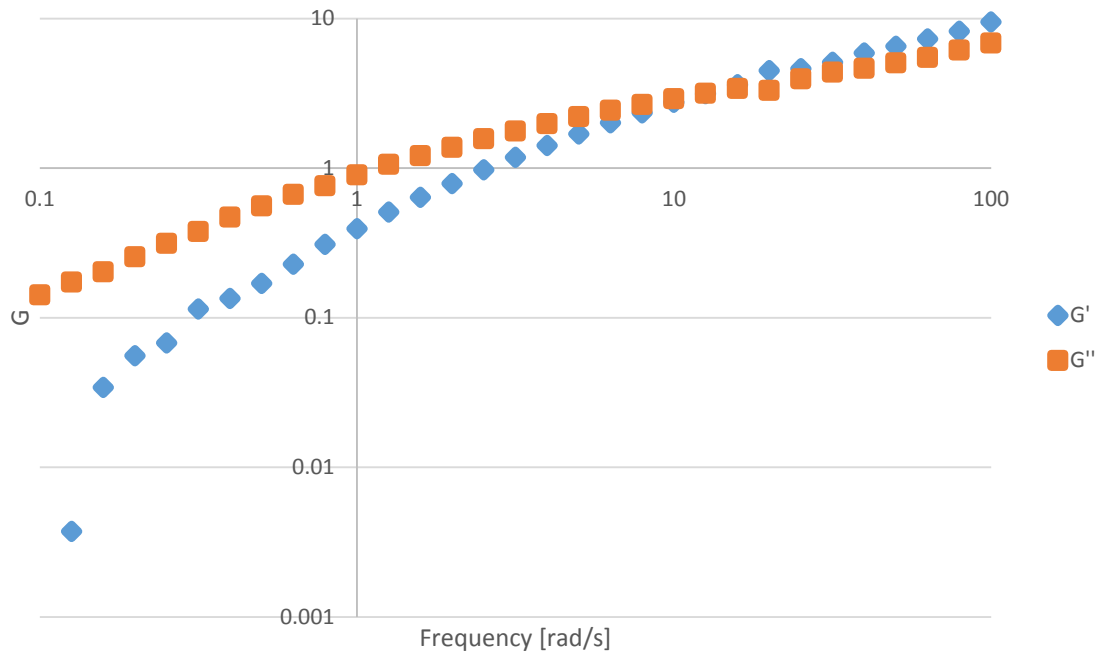


Figure 15. Storage and loss moduli of fracking fluid (0.5 % guar, 0.08 wt % sodium tetraborate solution).

3.2 Modeling settling velocity in fiberless fluid

It is critical to be able to predict what the settling velocity of particle would be for a given fluid. A classic example of such a predictive model is Stoke's Law, which emerges from a force balance of a sphere in a Newtonian fluid. Stoke's Law assumes that there are three forces acting on the settling sphere: gravitational, buoyant, and viscous drag. When the sphere reaches

terminal velocity, the velocity of the sphere could be calculated knowing that the gravitational force equals the buoyant and viscous drag forces [3]. The final expression for Stoke's Law is show in Equation 2 below

$$v = \frac{2(\rho_s - \rho_f)}{9\mu_f} gR^2 \quad (3)$$

However, because the viscosity of hydraulic fracturing fluids does not remain constant with shear, Stoke's Law is inadequate for predicting the settling velocity of particles in the fracking fluid. However, the simplest models that have been developed for modeling sphere sedimentation in non-Newtonian fluids have been created for power law fluids. For the sake of simplicity, hydraulic fracturing fluids were modeled as a power law fluid.

Previously, a model has been developed by Renaud et al. relating the flow index to the drag coefficient of a sphere settling in inelastic power-law fluid [13]. At low Reynold's numbers, it is well-known that the drag coefficient, C_D , can take the form of a Newtonian drag coefficient modified by some function, $X(n)$, which depends on the flow index of the power-law fluid.

$$C_D = \frac{24}{Re} X(n) \quad (4)$$

The form of $X(n)$ is obtained from a balance of the rate of energy dissipation of the fluid and by assuming that the average shear rate is also some function of the flow index.

$$\dot{\gamma}_{avg} = \alpha(n)\sqrt{6}v/d \quad (5)$$

$$C_D \frac{\pi d^2}{4} \frac{\rho_f v^2}{2} = m \left[\frac{\alpha(n) \sqrt{6} v}{d} \right]^{n+1} (3) \left(\frac{\pi d^3}{6} \right) \quad (6)$$

$$X(n) = \frac{[\sqrt{6} \alpha(n)]^{n+1}}{6} \quad (7)$$

Theoretical values of $X(n)$ have been calculated in the literature. From these calculations one can obtain correlations for α_n , and by using Equation 5 above, one can obtain an expression of $X(n)$ which depends solely upon the flow index of the fluid.

$$X(n) = (0.992 \pm 0.021) \frac{3}{n^2 + n + 1} \quad (7)$$

Furthermore, Graham et al have developed an empirical model derived from experimental correlations relating the drag coefficient to the particle Reynolds number in a power law fluid [11].

$$C_D = \frac{35.2}{Re^{1.03}} + n \left(1 - \frac{20.9}{Re^{1.11}} \right) \quad (8)$$

By setting Equations 4 and 8 equal to each other, one can solve for the Reynolds number. The Reynolds number could be related to the settling velocity in a power law fluid using the following well known expression

$$v = \left(\frac{kRe}{(d/2)^n \rho_f} \right)^{\frac{1}{2-n}} \quad (9)$$

This method was used to make predictions about the settling velocity. The results of these predictions are shown in Table 3.

Table 3. Predictions of settling velocity

Particle	Experiment	Stoke's Law	Stoke's Law Error (%)	Power Law	Power Law Error (%)
Aluminum	0.49	0.34	-31	0.52	6
PTFE	1.25	0.62	-50	0.94	-25

It can be seen from Table 3 that the power law method is an improvement over Stoke's Law. However, it still does not predict settling rate accurately enough. In order to more completely assess the validity of this power law method, it was used to predict the settling rates from previously obtained data sets. Figure 16 again shows that the power law method is an improvement over Stoke's Law. However, the power law method becomes increasingly less accurate as the crosslinker concentration is increased.

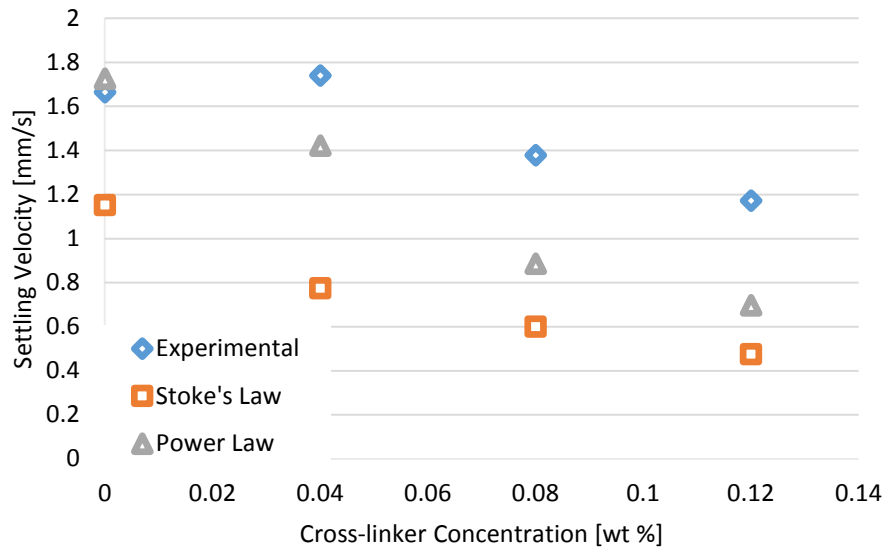


Figure 16. Settling velocity predictions for 0.5 wt % guar solution at varying sodium tetraborate concentrations. The particle is PTFE.

3.3 Modeling the effect of fibers

Of greater interest is to determine how fibers affect the settling velocity. In the system encountered in these experiments, there are four primary interactions: sphere-fiber, sphere-fluid, fiber-fiber, and fiber-fluid. Realistically, these interactions cannot be decoupled from each other. For example, the flow field generated by the sphere could disturb fibers and induce them to interact with each other, and the movement of these fibers could in turn disturb the flow field. However, for the sake of simplicity these interactions will be treated as independent of each other.

The velocity effects due to sphere-fluid interactions could be accounted for with the method described in section 3.2. The sphere-fiber interactions could be modeled as a basic mechanics problem, after assuming that the fibers do not undergo drag. The fibers were treated as a rigid rod which rotates about its center of mass and that the sphere always hits the fibers at the tip.



Figure 17. A schematic of the sphere-fiber interaction.

Assuming that the sphere imparts both translational and rotational momentum on the fiber, the final velocity of the sphere could be solved for using energy, angular momentum, and linear momentum balances. The energy balance is shown in Equation 10 below. m is the mass of the sphere, v_i is the initial velocity of the sphere, v_f is the final velocity of the sphere, m_c is the mass of the fiber, v_c is the translational velocity of the fiber, I_c is the moment of inertia of the fiber, and

ω_c is the angular velocity of the fiber. For a rigid rod, the moment of inertia is $I_c = m_c L^2/12$, where L is the length of the fiber.

$$\frac{1}{2} m v_i^2 = \frac{1}{2} m v_f^2 + \frac{1}{2} m_c v_c^2 + \frac{1}{2} I_c \omega_c^2 \quad (10)$$

The final translational velocity of the fiber could be written in terms of the final and initial velocities of the sphere using the linear momentum balance.

$$m v_i = m v_f + m_c v_c \quad (11)$$

And the angular velocity of the fiber could also be written in terms of the initial and final velocities of the sphere.

$$\frac{L}{2} m v_i = \frac{L}{2} m v_f + I_c \omega_c \quad (12)$$

After these substitutions have been made, the final velocity of the fiber could be calculated.

However, this only predicts what the velocity of the sphere is after hitting a single fiber. To find the total number of fibers the sphere hits, the number of fibers per unit volume of the sphere is found, and that is multiplied by the volume that the sphere has traversed.

$$N_{hit} = V_{travelled} \frac{N_{fibers}}{V_{total}} = N_{fibers} \frac{r_{sphere}^2}{r_{graduated\ cylinder}^2} \quad (13)$$

The final velocity of the sphere after hitting all these fibers are calculated in two ways. The first way is to calculate how much a sphere's velocity is reduced after hitting one sphere and multiply that by the number of fibers the sphere hits, and use that as the total velocity reduction for calculating the final velocity. The results of this calculation is shown in Figure 18 on the next page. The second method for calculating the final velocity is to do discrete calculations, that is after hitting one fiber, use the resulting sphere velocity for calculating the final velocity after hitting another fiber, and so on until all fibers have been hit. If the number of fibers hit is not an integer number, it is rounded up. The values used for the initial velocity are the predictions made using the power law method. The results for these calculations are shown in Figure 19 on the next page.

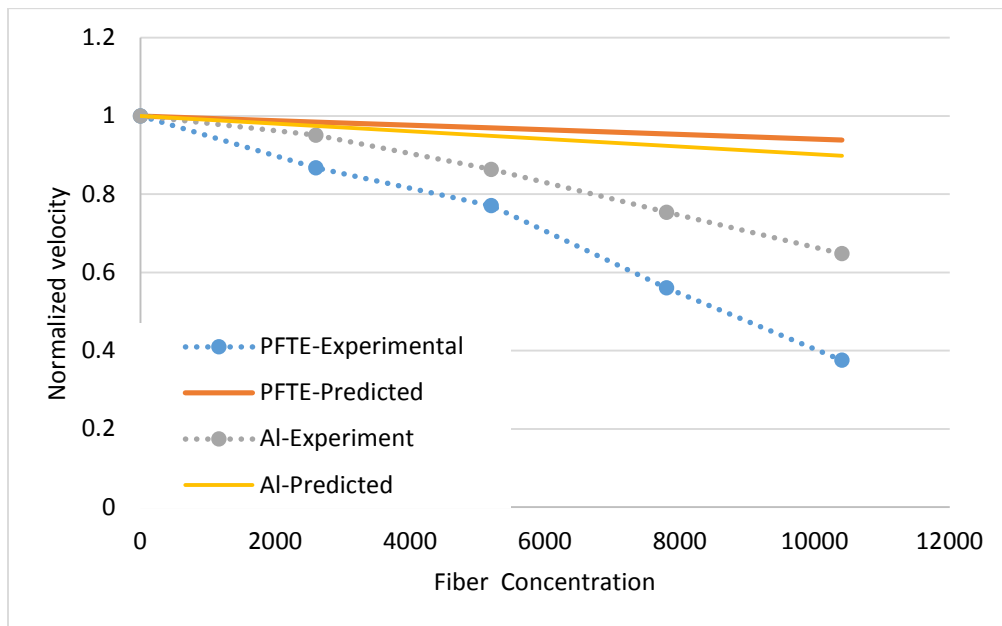


Figure 18. Bulk predictions.

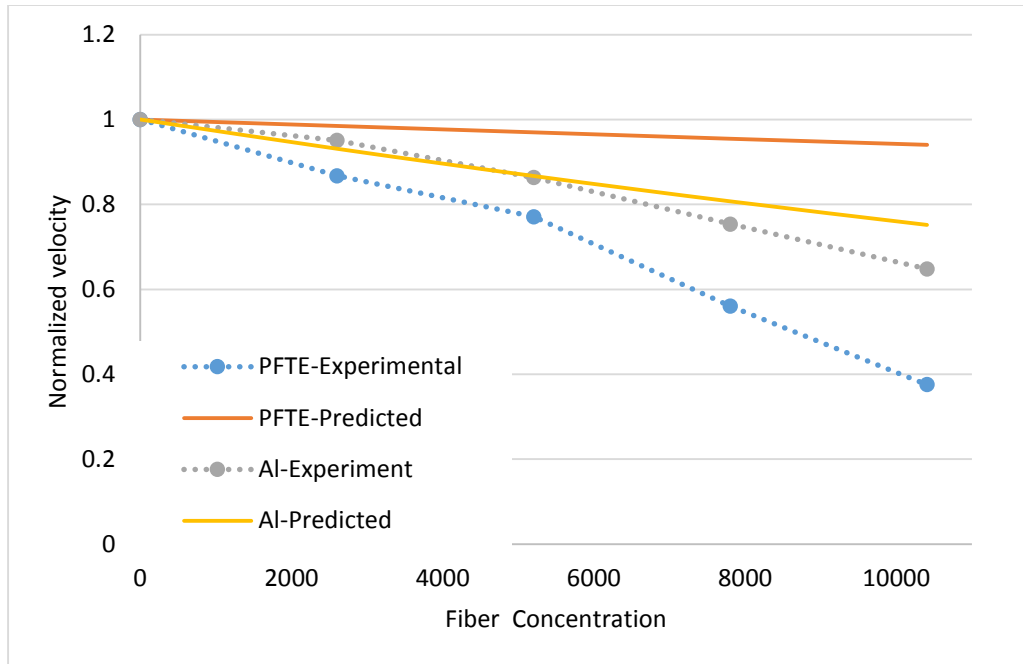


Figure 19. Discrete predictions.

It can be seen from Figure 18 and 19 that the discrete method works well in predicting the final velocity of the aluminum bead, but does badly in general. Furthermore with the discrete method, the prediction for the velocity of the PTFE bead became slightly worse. The PTFE bead has a larger diameter than the aluminum particle and hence a higher velocity. The PTFE bead generates greater disturbances in the fluid which become significantly affected by the fibers. This method of predicting final velocity is more accurate when the initial velocity of the sphere is lower. Furthermore, the assumptions made in the calculations could just be inappropriate. For systems with high fiber concentrations, one end of the fiber could be treated as trapped by the other fibers while the other end interacts with the sphere [10]. In this case, the fiber rotates about its tip instead of its center of mass. However, when the calculations were made using these assumptions, there was not a significant difference over calculations where the fiber was

assumed to rotate about its center of mass. And it can be seen from Tables 18 and 19 that both the bulk and the discrete predictions become increasingly worse at higher fiber concentrations, when fiber-fiber interactions become increasingly important. At these concentrated fiber suspensions, when the fiber could be treated as being trapped in one end, a particle with low momentum might move around the fiber and a particle with high momentum would reorient not only the fibers it comes into immediate contact with but also the those trapping the fibers the sphere comes into immediate contact with [14].

Chapter 4: Conclusions and Future Work

4.1 Conclusions

Settling velocity experiments were performed using 4 different fiber types at four different fiber concentrations. It was found that thin, 38 μm nylon fibers worked the best, even when compared to glass fibers, which is the industry recommended fiber type [15]. When using nylon fibers or glass fibers, it was found that greater concentrations of fiber decreased the settling velocity of the sphere. However for propylene fibers it was found that fiber concentration did not reduce settling velocity.

When the settling velocity was compared to the bending radii of the fibers it was found that the most effective fiber (38 μm nylon) had the lowest bending radius, and that the 4 mm polypropylene fiber, which essentially did not affect the settling velocity, had the highest bending radius. The bending radii is an estimate of how much a fiber bends when it makes contact with a moving sphere. In general it was found that fibers of increasing bending radii affect settling velocity less, and that the effects of fiber concentration become less important at higher bending radii. Thus in actual fracking applications it would be more ecologically and economically efficient if fibers with lower bending radii were used since it will allow for lower fiber concentrations to be used.

A simplistic model was also created for predicting the settling velocity of a sphere in fiber-filled fluid. It was assumed that the two primary contributors to settling velocity were the sphere-fluid interactions and the sphere-fiber interactions. For determining the velocity due to sphere-fluid interactions, hydraulic fracturing fluid was treated as a power-law fluid. A method was devised to determine the settling velocity of a sphere once the properties of the fluid are known. It was

found that this method was an improvement over Stoke's Law, but that it still did not predict settling velocities accurately particularly at higher cross-linker concentrations or for systems which intrinsically have higher settling velocities. This method ignores the viscoelasticity of the fluid, which is possibly why the predictions get worse as the cross-linker concentration is increased. Also, the assumption behind the equations used for this method was that the fluid is in the creeping flow regime. When a particle is used which naturally results in higher settling velocities, this method is expected to become less accurate. Also it can be concluded from this research that the sphere-fiber interactions alone are insufficient to account for the effects of fibers on settling velocity.

4.2 Future work

It is recommended to do experiments using proppants to determine whether the results found so far, particularly with the trends for the settling velocity and bending radii, are adaptable for systems in bulk. It is also recommended to find a better method for calculating the settling velocity of spheres in fracking fluids, preferably one that accounts for the viscoelasticity of the fluid. It is also recommended to incorporate fiber-fiber and fiber-fluid interactions into models accounting for the fiber effects on settling velocity. Also, these different interactions should not be treated as independent of each other.

References

- [1] “Unconventional Gas Shales: Development, Technology, and Policy Issues”. Congressional Research Service. 30 October 2009.
- [2] Sitdikov, S.; Serdyuk, A.; Nikitin A.; Yudin, A.; Mullen, K.; Oussoltsev D.; Butula, K.K. “Fiber-Laden Fluid—Applied Solution for Addressing Multiple Challenges of Hydraulic Fracturing”. Society of Petroleum Engineers. 2009.
- [3] Elgaddafi, Rida; Ahmed, Ramadan; George, Matthew; Growcock, Fred. “Settling behavior of spherical particles in fiber-containing drilling fluids”. *Journal of Petroleum Science and Engineering*. Web. 7 February 2012.
- [4] Sharma, Mukul M.; Bonnecaze, Roger; Norma, Jay; Liu, Yajun; Gadde, Phani B. “Modeling Proppant Settling in Water-Fracs”. Society of Petroleum Engineers. 2004.
- [5] "Description: Hydraulic Fracking." *OilPatchCopyWriter*. Web. n.d.
- [6] Barati, Reza; Liang, Jenn-Tai. “A Review of Fracturing Fluid Systems Used for Hydraulic Fracturing of Oil and Gas Wells”. *Journal of Applied Polymer Science*. 2014.
- [7] 7, Johannes. *Oil Field Chemicals*. 2003. Gulf Professional Publishing. Digital file.
- [8] Gauthier, Joseph. “Rheology and Settling Dynamics of a Particle-filled aqueous polymer gel for hydraulic fracturing fluid systems”. Thesis. The Ohio State University, 2014.

- [9] Ohanian, Nicholas. “The Examination of Fiber and Breaker Effects on the Rheological and Settling Rate Characteristics of Hydraulic Fracturing Fluids”. MS Thesis. The Ohio State University, 2014.
- [10] Harlen, Oliver; Sundarajakumar, R.R.; Koch, Donald, L. “Numerical simulations of a sphere settling through a suspension of neutrally buoyant fibers”. *Journal of Fluid Mechanics*. Web. 1999.
- [11] Graham, D., & Jones, T. (1994). “Settling and transport of spherical particles in power-law fluids at finite Reynolds number”. *Journal of Non-Newtonian Fluid Mechanics*, Vol. 54, 1994, pp. 465-488.
- [12] Mackosko, Christopher W. *Rheology Principles, Measurements, and Applications*. New York: Wiley-VCH, 1994. Print.
- [13] Renaud, Maruice; Mauret, Evelyne; Chhabra, Rajendra. “Power-Law Fluid Flow Over a Sphere: Average Shear Rate and Drag Coefficient”. *The Canadian Journal of Chemical Engineering*. Web. 2004.
- [14] Antonio, David; Chaouche, Mohend. “Sedimentation of a sphere in a suspension of neutrally buoyant fibers”. *Journal of Rheology*. Web. 2002.
- [15] Armstrong, Kevin; Card, Roger; Navarrete, Reinaldo; Nelson, Erik; Nimerick, Ken; Samuelson, Michael. “Advanced Fracturing Fluids Improve Well Economics”. *Oilfield Review*. Web. 1995.